Core-shell structure in self-assembled lead/lead-oxide nanoclusters revealed by photoelectron spectroscopy

Chaofan Zhang, Tomas Andersson, Svante Svensson, and Olle Björneholm
Department of Physics and Astronomy, Uppsala University, P.O. Box 530, 75120 Uppsala, Sweden

Maxim Tchaplyguine
MAX-lab, Lund University, P.O. Box 118, 22100 Lund, Sweden

(Received 28 September 2012; published 2 January 2013)

Nanoclusters containing metallic lead and lead oxide have been produced by self-assembly out of a primary mixture of lead atoms and oxygen in a reactive sputtering-based cluster source. Comparison of the valence and core-level responses in the photoelectron spectra shows that clusters have a core-shell structure with a lead-oxide core coated by an outer shell of metallic lead. This core-shell order is opposite to that typical for most microscopic and macroscopic materials. We explain this by the peculiarities of the cluster production kinetics and by the system's energy minimization striving due to what lead oxide is placed in the core of the mixed cluster.

DOI: 10.1103/PhysRevB.87.035402 PACS number(s): 61.46.Bc, 36.20.Kd, 73.40.Ns, 75.20.En

I. INTRODUCTION

Nanomaterials consisting of group-IV elements or/and their oxides are intensively studied as possible building blocks for novel nanoscale semiconductor devices and superconductive materials.[1–6] Substantial efforts have been spent to unveil the transition from conductor to semiconductor properties in the group-IV metals at nanoscale.[2,7–10] Recently one of the most modern and advanced experimental tools, the free electron laser, has been implemented to probe the metal to nonmetal transition in Pb clusters, predicted by the theoretical calculations[11,12] at the size of about 20 atoms.[9] By tailoring the size of group-IV metal nanoparticles, it may become possible to create systems in which core-shell structures have radial segregation of conducting/semiconducting properties. To approach a similar goal from a somewhat different direction, many works have been performed on the system with specific properties appearing due to the oxide surface layer grown on metallic nanoparticles, nanowires, nanobelts, and nanotubes.[13–15] Core-shell structures of Sn/SnO_2 nanowires similar in properties to those of Zn-ZnO have been fabricated in a thermal oxidization process.[16,17] Lead-oxide nanotubes filled with metallic lead have also been synthesized by thermal evaporation.[18] In all the cases mentioned above and many others, the structures were created with the metal covered by its oxide, which is also common for macroscopic materials. In this study, free nanoscale clusters containing metallic lead and lead oxide have been produced, and their core-shell structure with the oxide in the bulk and metallic layer on the surface has been established using information on the cluster electronic structure obtained by x-ray photoelectron spectroscopy.

Nanostructures with a semiconductor interior and a conducting monolayer on the surface are now probably among the most studied objects in solid-state physics. The main emphasis here is on the so-called topological insulators usually built on the basis of one of the poor metals like bismuth or antimony. Nanoparticles of the type created in the present work resemble topological insulators in the sense of the conductivity geometry and can be discussed in the context of the same potential applications. Another interest in conquering a simple technique of covering oxide nanoparticles with a metallic monolayer can be in the possibility to encapsulate the unstable oxides, such as of gold, for their consequent studies.

The present study on clusters/nanoparticles of a complex composition starts out from the ideas to form them in a beam by a self-assembling process, thus avoiding any influence of a substrate, and also to probe the resulting clusters "in-flight" in the same beam. In this work, the clusters have been created via aggregation of a multicomponent primary vapor mixture. This technique has been implemented in our earlier study of NaK nanoalloy clusters[19] and several studies of the inert gas clusters with a mixed composition.[20–22] In these earlier studies, the radially segregated structure formation in the self-assembling process has been explained mainly by the difference in the cohesive energies of the components,[21] due to what the core-shell structure has been formed with the high cohesive energy component in the interior and the low cohesive energy component on the surface. For all the studies mentioned above, the structure of the bicomponent clusters could be established by analyzing the change in the ratio of the well-resolved surface and bulk responses and the changes in their energies in the core-level photoelectron spectra. Since lead does not exhibit such well-separated bulk and surface features, in the present study we have used the photoelectron angular distribution (PAD) for the lead/lead-oxide clusters to unveil their internal spatial structure.

PAD has been shown to be an informative channel for distinguishing the responses from different sites of a nanoscale system.[23–25] This method works when the distribution of photoelectrons is highly anisotropic. For example, in the case of Ar 3*s*-level ionization of a single separate atom, there are no electrons ejected and consequently detected in the direction perpendicular to the polarization plane of the ionizing radiation. However, this is different for argon clusters, especially for the photoelectrons emitted from the bulk atoms.[25] Their angular distribution becomes much more isotropic due to the elastic scattering effect: in the process of escaping from the clusters, the bulk photoelectrons become rather uniformly distributed in all directions. The angular distribution of photoelectrons is usually characterized by the

so-called anisotropy parameter—the β parameter.[26] Elastic scattering of bulk photoelectrons on the lattice ions and electrons leads to a much more isotropic PAD and thus a lower value of the β parameter for the bulk atoms compared with that of the surface atoms.[23–25] As it will be shown below, the differences between the PAD β parameters for the different electronic levels used in the studies allow us to make qualitative judgments on the geometry structure of lead/lead-oxide clusters.

II. EXPERIMENT

The lead/lead-oxide clusters have been produced by gas aggregation with magnetron-based sputtering creating the primary vapor of metal atoms.[27,28] The schematics of cluster production is shown in Fig. 1. The method has been used earlier by us to produce large-size metal clusters (with the diameter below 10 nm, corresponding to the mean size of 10^3 to 10^4 atoms).[29–32] In the present experiments, the metal vapor was created by sputtering a pure lead target of a 50-mm diameter and 6-mm thickness. Argon gas has been used as for sputtering as well as for the cooling of the lead vapor. Argon input pressure has been kept at ≈5 mbar set by a high-precision leak valve and measured by a gas-independent gauge. In the present gas-aggregation source, the magnetron is placed inside a stainless-steel cryostat, which ends in a copper nozzle with a channel of 2-mm diameter and 20-mm length. The cryostat has double walls, and liquid nitrogen is continuously let through the volume between the walls. It is possible to keep the cryostat temperature close to that of liquid nitrogen, while sputtering powers reach up to 300-W dc. The cryostat is installed inside a vacuum chamber where the pressure during the operation is, as a rule, in the 10^{-4} mbar range. As briefly mentioned above, in such a source the clusters are formed by vapor condensation in collisions between metal atoms and cold buffer gas atoms inside the cryostat volume. The flow of the buffer gas transfers the clusters from the cryostat through its nozzle into the ionization volume, where the clusters are irradiated by the synchrotron light. Before entering the ionization volume, the cluster beam from the cryostat passes through a conical skimmer with a 2-mm-diameter orifice.

Additionally, in the present experiments, helium gas has been let into the cryostat from a separate gas line ending at the rear wall of the cryostat. This allowed us to increase the mass flow through the cryostat without influencing the discharge plasma parameters significantly and thus to increase the cluster response. Helium input pressure has been kept at ≈10 mbar set by a high-precision leak valve and measured by a gas-independent gauge. In our earlier studies on metallic lead clusters produced by the present cluster source,[32] it has been established that mostly neutral nanoparticles were formed at the magnetron discharge powers below 200 W. In the present studies of the valence and 5*d* levels of lead, the power has been kept at 100 W, with the discharge current of ⩽0.4 A. For recording Pb 4*f* spectra, the power has been increased to 140 W, 0.5A current. Comparison of Pb 5*d* cluster spectra of clusters produced with 100-W and 140-W power did not show any significant differences of the spectral shapes in this range of discharge parameters.

To create nanoclusters containing metal oxide, the so-called reactive sputtering has been implemented in the present experiments. This method is known to produce various lead oxides with different oxidation states, depending on partial oxygen concentration in the discharge.[33] In the present experiments, the argon gas, injected in the setup directly in front of the sputtering target, has been mixed with oxygen before entering the cryostat. Oxygen has been let into the argon gas line via a separate high-precision leak valve. The mixing ratio has been varied in a range between ≈2 and ≈15% (keeping argon input pressure constant), allowing us to change the response of the clusters from pure metallic to pure oxide. The details are discussed below.

The experiments have been carried out at beamline I411 at the Swedish national synchrotron radiation facility Max-lab in Lund, Sweden. The beamline delivers horizontally polarized radiation in the range from 40 to ∼1000 eV. The cluster source has been attached to the permanent endstation of the beamline. The rotatable ionization chamber of the endstation is equipped with a Scienta R 4000 electron energy analyzer, which for the PAD study in the present experiments, has been placed at two angles (first at 90° and then at the so-called "magic angle" of 54.7°) with respect to the horizontal polarization plane of the radiation. In the case of 90°, to a great extent only those

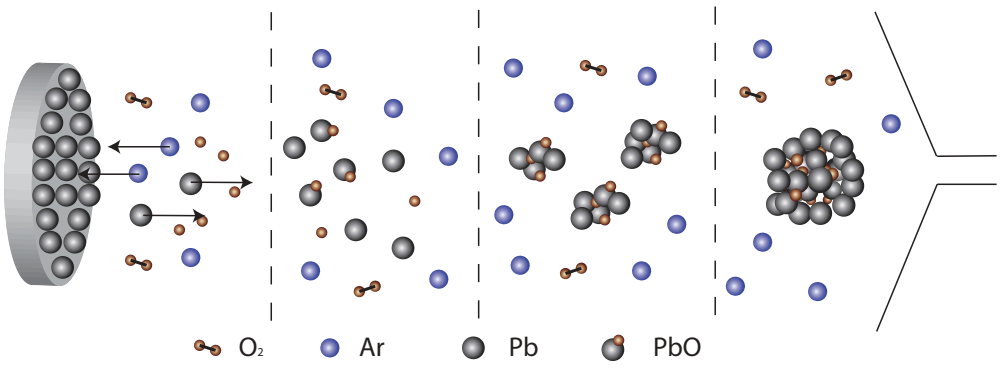

FIG. 1. (Color online) The schematic figure of the clusters production. The clusters are produced by the gas-aggregation method using the magnetron sputtering. When oxygen is let in the cryostat, a part of lead atoms form lead-oxide molecules, and then the mixed lead/lead-oxide clusters are created in the aggregation process. At a later stage of the flow through the cryostat, no dissociated oxygen is left, and a metallic layer is deposited on clusters.

photoelectrons that were emitted from the ionization volume perpendicularly to the polarization plane were detected by the spectrometer. The collection angle of the spectrometer has been about 10° along the photon beam direction and below 10° perpendicular to it. Cluster valence levels as well as the regions of lead $5d$ and $4f$ core levels have been probed with photon energies providing the maximal ionization cross sections for the corresponding electronic states: ≈40 eV for the valence, ≈50 eV for the $5d$, and ≈250 eV for the $4f$. The $5d$ and valence binding energy scale has been calibrated using the $3p$ level of atomic Ar present in the beam from the cryostat. The $4f$ spectra have been calibrated using Kr $3d$ spectra. In the photoelectron spectra, the total experimental resolution has been around 0.1 eV in the $5d$ photoelectron region and ≈0.2 eV in valence and $4f$ regions.

III. RESULTS AND DISCUSSION

A. Photoelectron spectra of Pb 5*d* and valence levels

For each clustering condition—determined mainly by argon, helium, and oxygen concentrations—the photoelectron spectra of the valence region and of lead $5d$ core levels have been recorded first with the analyzer at 90° with respect to the polarization plane of the radiation. Before letting oxygen into the magnetron discharge volume, the pure metal clusters have been produced, and their response has been characterized. In the left panel of Fig. 2, case A shows the $5d_{5/2}$ spin-orbit component of the photoelectron spectrum of metallic lead clusters. This spectrum resembles in energy and shape that of macroscopic lead and of large Pb clusters studied by us

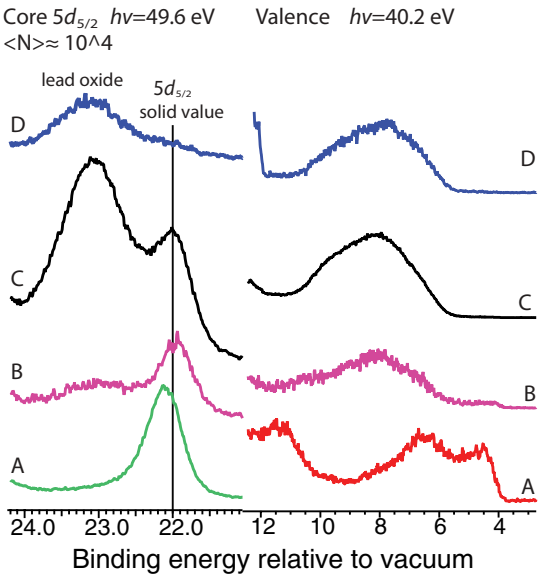

FIG. 2. (Color online) Photoelectron spectra of Pb/Pb-oxide mixed composition clusters. Left panel: the $5d_{5/2}$ core-level region. Right panel: the valence region. Case A: $5d$ and valence photoelectron spectra of metallic lead clusters. Cases B to D: Oxygen is let into the cryostat (see text for the details); the ratio of lead oxide increases in the Pb/Pb-oxide mixed-composition clusters. All the spectra recorded with the analyzer placed at 90° relative to the electric polarization vector.

earlier.[32] The $5d_{5/2}$ cluster binding energy is only ≈0.1 eV higher than the 22.0-eV value of the "infinite" solid. Applying the so-called conducting sphere approximation,[34] one can estimate the average radius and the average number of atoms of the distribution of sizes in the cluster beam. For the metallic lead clusters [Fig. 2(a)], the estimated radius is 6 to 7 nm, indicating that the number of atoms per clusters is in the 10^4 range, if the clusters have the same density as the solid. Having characterized the response of metallic lead clusters, we have proceeded to the next step to stepwise introduce oxygen into the cryostat. Oxidation of metal atoms and clusters in the reactive sputtering process is facilitated by the conditions of magnetron discharge plasma. Near the target, oxygen is either dissociated and/or excited and/or ionized to a great extent. As briefly mentioned above, reactive dc magnetron sputtering of lead is known to create different types of oxides from the series PbO, Pb_3O_4, Pb_2O_3, and PbO_2.[33]

When oxygen was introduced into the cryostat, a spectral feature at a binding energy about 1 eV above that of metallic lead appeared [Figs. 2(b) to 2(d), left panel]. The binding energy separation of this extra feature from the metallic lead response was consistent with the values for macroscopic lead oxides.[8,35] The relative intensity in the oxide $5d$ region increased with the increasing oxygen fraction in the sputtering gas. At a certain oxygen concentration, ∼15% relative to argon ($P_{Ar} \approx 5$ mbar), the contribution of the metallic lead signal became very weak in the $5d$ region [Figure 2(d)), left panel)]. For recording spectrum B, where the metallic response is stronger than that of lead oxide, the oxygen input pressure has been kept at 2–4% relative to argon. For spectrum C, where the metal-to-oxide intensity ratio reversed, the oxygen input pressure has been increased to 8–10% relative to Ar. All these $5d$ spectra recorded at different oxygen concentrations give a reliable basis to claim that clusters containing lead oxide have been produced in the reactive magnetron sputtering process. This conclusion is supported and extended by our observations in the valence region.

The valence photoelectron spectra, shown in the right panel of Fig. 2, were recorded at the same clustering and acquisition (90°) conditions as for the $5d$ spectra in the left panel of the figure. The metallic lead clusters (case A) exhibit a spectrum practically identical to that of macroscopic polycrystalline lead.[35,36] The spectral shape reflects the electron density of states with the Fermi edge at ≈4.0 eV. Not only the lower-energy feature due to the $6p$ electrons split into two subbands is seen, but also the band due to the $6s$ electrons between 11- and 12-eV binding energy is seen.

In the valence spectrum of case B, when oxygen (2–4% relative to argon) was let into the cryostat, the metallic lead cluster feature became weak, and a strong structureless band showed up between 6 to 10 eV. We assign this spectrum to be the valence-band response of the clusters containing lead oxide. Indeed, corresponding band shapes have been observed in multiple studies of macroscopic lead oxide, for example.[35,36] (Moreover, as it will be discussed below, the shape of the valence band of lead oxide allows us to make a conclusion on the degree of oxidation.)

In case B, one notices a dramatic difference in the intensity ratio of lead oxide to metallic lead between the $5d$ and the valence spectra. The lead-oxide response is dominant in the

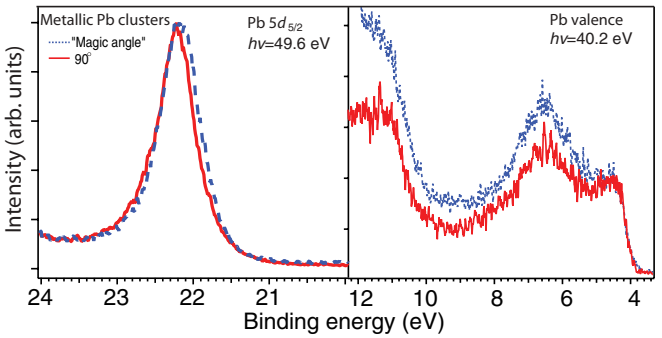

FIG. 3. (Color online) Pb $5d_{5/2}$ (left panel) and valence (right panel) level photoelectron spectra of metallic Pb clusters; the dashed-line spectra have been recorded at the "magic angle" and the solid ones at 90°. The valence spectra have been normalized to the lower-energy $6p_{3/2}$-related part of the valence band.

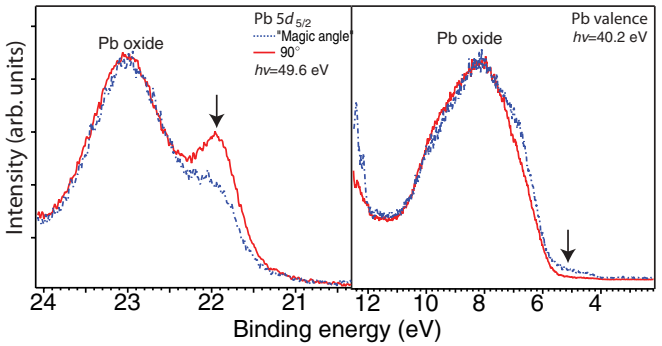

FIG. 4. (Color online) The Pb $5d_{5/2}$ (left panel) and valence (right panel) level photoelectron spectra of mixed-composition Pb/Pb-oxide clusters; the dashed-line spectra have been recorded at the "magic angle" and the solid-lines at 90°. The spectra have been normalized to the Pb-oxide peaks. In the left panel, the 5*d* spectrum recorded at 90° has a higher ratio of metallic Pb to Pb oxide in the mixed-composition clusters. In the right panel for the valence, it is the opposite: the metallic response is stronger in the "magic-angle" case.

valence spectrum (right panel B), while in the corresponding 5*d* spectrum (left panel B), it is the metallic response that is much stronger. When more oxygen is added (8–10% relative to argon; case C), we can hardly see any response of metallic lead in the valence region, whereas the 5*d* signals from metallic lead and lead oxide are comparable in intensity. In the extreme case D, with even more oxygen (13–15% relative to argon), finally also the metallic response in the 5*d* region becomes weak but still clearly detectable. The metallic valence signal is not seen even at a considerable enlargement of the intensity scale. This apparently contradictory behavior of the 5*d* and valence signals are a clue to the internal structure of the clusters. We interpret the observed changes in the relative intensity of lead and lead oxide as due to the interplay between the spatial distribution of constituents and the significantly different PADs for the valence and for the 5*d* levels. While the 5*d* electrons have a rather isotropic angular distribution, the valence electrons are ejected mainly perpendicular to the observation direction. As discussed in the Introduction, this leads to a different representation of the cluster surface and bulk by the valence and by the 5*d* photoelectrons.

Analogous measurements of lead 5*d* and valence spectra at different oxidation conditions have been performed at the "magic" angle. These spectra should be much less influenced by the angular effects than those obtained at 90°: the surface sensitivity of the valence and 5*d* spectra should be similar, as will be discussed in detail below. Figure 3 shows the metallic-cluster spectra at similar clustering conditions for both angles: 90° and ≈54.7°. The 5*d* spectra are seen to be practically identical in their spectral shape, so no special normalization has been necessary. The valence spectra have been normalized to the lower-energy $6p_{3/2}$-related part of the valence band. The intensity, which can be attributed to the $6p_{1/2}$ electrons (between 6 and 7 eV), is somewhat higher at the "magic angle"; however, the difference can be explained by the steeper rising but not exactly known background. For the oxidized clusters (8–10% O_2 relative to Ar in the gas mixture), the valence spectra recorded at 90° (the same as case C in Fig. 1) and 54.7° differ in principally important details (see Fig. 4, right panel). The metallic part is absent at 90° and is clearly seen at 54.7° between 4 and 7 eV in Fig. 4. At the same time, in the corresponding 5*d* spectra, the situation is the opposite: it is at 90° where the metallic response is stronger.

B. Core-shell structure derived from PAD

The spectral behavior, illustrated by Figs. 2–4, is consistent with only a certain structure of the clusters produced in the self-assembling process. First of all, we make a claim that not separate metallic and lead-oxide clusters are produced but mixed-composition clusters containing both metallic and oxide regions. Formation of separate clusters is, in general, unlikely at such conditions, and this consideration is confirmed by the recorded spectra. Indeed, spectral manifestation of separate metallic and fully oxidized nanoparticles would be different relative to what we have observed: The intensity ratio of the lead/lead oxide would be about the same for the valence and for the 5*d* level response—at each oxygen concentration. This is especially true for the present choice of photon energies. Indeed, the kinetic energy of the valence and 5*d* photoelectron is practically the same in our experiments; thus, the electron escape depth is the same, so the corresponding valence and 5*d* signals would represent the number of atoms per cluster in a similar way. We conclude that clusters of a complex composition are formed.

For the lead valence levels, PAD studies[37] revealed that the angular anisotropy parameter β at the 40-eV photon energy is close to 2.0, meaning that there are hardly any electrons ejected at 90° with respect to the polarization plane. However, as mentioned in the Introduction, in the case of clusters, the effective β for the same level can be considerably lower than for separate atoms, due to the elastic scattering of the photoelectrons coming out from the cluster interior up to the surface. The angular distribution of such bulk photoelectrons appears to be much more isotropic, making it possible to detect them even when the spectrometer is placed perpendicular to the radiation electric vector. For the surface electrons, the angular distribution is much less affected by elastic scattering and is atomiclike,[23] so the valence electrons will be coming out from

the clusters still in-plane with the polarization vector and will not be detected by the spectrometer at 90°. As the result, the lead valence signal collected at 90° is much more bulk sensitive than that recorded at the magic angle.

For the 5*d* level on the other hand, the atomic anisotropy parameter is quite small (≈0.5) at the 50-eV photon energy.[38] Thus, the distribution of electrons is rather isotropic from the very moment of ejection and is similar for the photoelectrons that escaped from the bulk and from the surface. In view of these considerations, the dominating signal from metallic lead in the 5*d* spectrum [Fig. 2(b), left panel] and the simultaneously much stronger lead-oxide signal in the valence spectrum [Fig. 2(b), right panel] can be explained by the presence of mainly metallic lead on the cluster surface and lead oxide in the cluster interior. The clusters we have produced are nanoparticles with the core-shell structure in which a lead-oxide core is covered by metallic lead. This order is opposite to what is typical for macroscopic materials, or even for most of the nanoscale structures, where it is the metal that is covered by an oxide layer.

This reversed core-shell order occurs even when we have less lead oxide in the clusters—judging from the 5*d* spectrum B in Fig. 2—the spectrum reflecting the relative concentration of the bulk and surface atoms. The change in the lead/lead-oxide relative intensity within the 5*d* spectra—from type B to type C (Fig. 2, left panel)—can be explained by the presence in case B of metallic lead areas also under the surface and first of all in the second monolayer. Indeed, at the kinetic energies in question, the electron escape depth is just few monolayers, so what we see in the spectrum is, to a great extent, the reflection of the structure of the outermost part of the clusters. If the oxide were too deep in the cluster, we would not be able to see the electrons from it. Alhough there is no experimental information for the deeper cluster-core composition, it is unlikely that the core becomes metallic again closer to the center. Naturally, in the case of a high oxygen concentration in the cryostat (spectra D in Fig. 2), the response of metallic lead in the mixed clusters decreases to nearly nothing even in the 5*d* response, also the surface layer is oxidized.

The 5*d* and valence spectral behavior with the acquisition at 54.7° is consistent with the geometric structure suggested above. Case C of the clustering conditions (Fig. 2) is the most illustrative here. For these conditions the spectra recorded at 90° and at the magic angle are compared in Fig. 4. At the magic angle the highly anisotropic flow of electrons from the cluster metallic surface becomes detectable, while at 90° the electrons from it are not seen (Fig. 4). At the same time for these clustering conditions, the metallic response in the 5*d* spectrum is more pronounced at 90° than at 54.7°.

Summarizing the above considerations on the lead/lead-oxide distribution in the clusters, one can conclude that when ≈2–4% O_2 is admixed into argon, not only the surface monolayer is metallic but, with a high probability, also the monolayer right under it. When oxygen concentration increases to 8–10%, only the outermost monolayer is not oxidized. When there is more than ≈13% O_2 in the sputtering mixture, the whole cluster consists of lead oxide.

In a gas-aggregation source, the cluster formation takes place over the whole distance from the primary vapor source to the very exit of the cryostat (about 15 cm in our case). This distance, known also as the aggregation length, has shown to be an important factor defining the cluster size for a magnetron-based source.[39] It is intuitively obvious and has been experimentally confirmed[39] that the longer the cluster stays in the cold vapor, the larger it becomes. Closer to the target, the magnetron discharge plasma is much richer in charged particles than further away toward the cryostat exit. The high ion and electron concentration leads to oxygen excitation, dissociation, and ionization, thus increasing its reactivity. It means that oxidation of the metal is significantly more probable in the vicinity of the target. The clusters, born first as agglomerates of oxide molecules, are swept downstream, into the regions where oxidation is less likely, but where the Pb atomic vapor, getting colder and colder further away from the target, is still present. This kinetics scenario can indeed lead to the core-shell structures with the oxide core and metallic surface.

Additionally, in such a gas-aggregation cluster source, a certain mobility inside the clusters is preserved within the formation time so that lowest-energy cluster stoichiometry can be achieved. It is energetically more favorable to place a constituent with weaker interatomic bonds on the surface of the clusters and to have the one with the stronger bonds in the bulk.[19] For clusters consisting of two similar types of atoms, such as clusters out of inert gases or alkali metals studied by us, one can discuss the formation energetics in terms of cohesive energies. For example, in the mixed Ar/Ne or Ar/Xe clusters, the cohesive energy of Ar is larger than that of Ne but smaller than that of Xe. Therefore, Ar occurs on the surface in the mixed Ar/Xe clusters but in the bulk of Ar/Ne formed in the self-assembling process.[22] Similarly, the low-cohesive energy component K is found to cover the surface of mixed Na/K nanoalloy clusters.[19] For the binary system lead/lead oxide, the considerations of the energy minimum principle should work in a more complex but qualitatively similar way. The melting temperature T_m of lead oxides is considerably higher than that of metallic lead (for Pb, $T_m = 327\,^{\circ}\mathrm{C}$; for Pb_3O_4, $T_m = 500\,^{\circ}\mathrm{C}$; and for PbO, $T_m = 888\,^{\circ}\mathrm{C}$), which means that the bonding within all types of lead oxide is much stronger than between the atoms of metallic lead.

For completeness, we should mention here the earlier relevant results on the segregation in bicomponent systems reviewed and discussed in Ref. 40. There, the surface energy of liquid Pb metal has been reported to be considerably smaller than that for liquid PbO, with the latter at ∼1200 K. This should, in principle, mean that in the liquid solution of metallic lead and PbO lead oxide, the element with the smaller surface energy—the metal oxide—would be segregated to the surface. Thus, it would be the order opposite to the one formed in the present work. This review[40] discusses the importance of thermodynamic and boundary conditions for the surface energy, which strongly depends on the temperature, and for compounds—on the atomic packing. The extrapolation of the conclusions made for the liquid to the solid phase is also mentioned to be not straightforward. There have been examples discussed in Ref. 40, such as the Cu-Au system, in which different model assumptions gave different predictions for the surface segregation. Referring these considerations to our results, one can probably reason here that in our production setup, all the different mechanisms competing with each other

at a certain time scale make the winner that stoichiometry that we observe.

C. Determination of the oxidation degree

The studies of the Pb $4f$ level of the clusters is of specific significance since it gives the possibility to compare the cluster spectra with those of macroscopic Pb oxides, for which most of the measurements have been performed for this very level.[8,35,36,41] The binding energy separation between the metallic lead and lead-oxide core-level spectral responses has always been the ground for the judgments on the degree of oxidation. However, the natural experimental difficulty here has been in the absence of a clear, common zero-energy point for comparison, when the sample was oxidized over the whole volume. There has been a discussion on macroscopic lead oxides, concerning whether PbO or PbO_2 had lower binding energies.[36,40] Reference 41 supports the conclusion that the higher degree of oxidation is, the lower the binding energy should be. In other words, the higher oxidation states would be closer to the metallic lead response in the spectra. In the present work the separation between the metallic lead and the oxide features is about 1 ± 0.1 eV for both the $4f$ (Fig. 5) and the $5d$ states. Depending on which work one relies on, such a separation would mean opposite assignments—either to PbO or to PbO_2. However, the situation is saved by the possibility to record a valence spectrum, serving as an additional and less ambiguous argument for the assignment. In Ref. 42 the PbO_2 valence spectrum exhibits two clear maxima, similar to metallic macroscopic lead and to the metallic lead clusters in the present experiments. For the clusters containing lead oxide, the spectra recorded by us have no such clear structure, but rather resemble those for PbO and Pb_3O_4—oxides with a lower degree of oxidation.[35,43,44] Taking this observation into account, we conclude that a smaller binding energy separation from the metallic lead response corresponds to

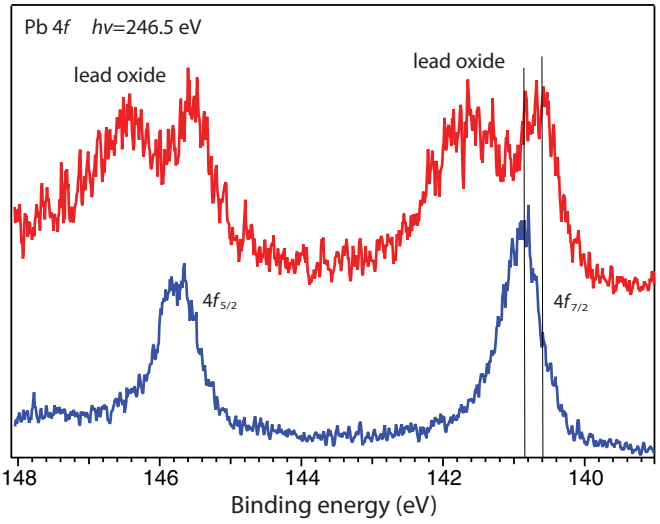

FIG. 5. (Color online) The photoelectron spectra of Pb $4f$ core-level ionization: the upper one corresponds to the case of mixed lead-oxide/lead-metal clusters; the bottom one is that of pure metallic lead clusters. The shifts between the metallic lead in two cases (marked by the solid lines) are due to the size differences.

PbO and/or Pb_3O_4. Such a conclusion has been made also in Ref. 36 and is in accord with the results on lead reactive sputtering.[33]

Assuming that there is one oxygen atom per lead atom (PbO) or about it (Pb_3O_4) in the whole nanoparticle, except for the surface one to two monolayers, it is possible to make an estimate of the cluster volume when it consists of the oxide. As mentioned in the experimental part, the radius of metallic clusters produced at the present sputtering conditions in the absence of oxygen is ≈7 nm. Using the macroscopic metallic lead atomic density, one gets $\approx 5 \times 10^4$ atoms per cluster for such a radius. The first approximation can be that in an oxidized cluster; about the same amount of lead atoms is present as in a typical metallic cluster. Using PbO macroscopic density, one can estimate the number of Pb-O pairs per unit volume. From that, one obtains the volume occupied by the same number of Pb-O pairs as there are atoms in the metallic cluster with $R \approx 7$ nm. The oxidized clusters appear to have 30% larger volume than the corresponding metallic ones. This percentage should not change significantly for different conditions studied in the present work, since the fraction of the surface monolayer atoms (one or two outermost layers) is small relative to the total number of constituent atoms, when the number is in the 10^4 range.

Finally, one can say that the 40% higher sputtering power used for getting a sufficiently intense $4f$ signal of lead-oxide-containing clusters created a correspondingly higher metal vapor concentration [at the same oxygen flow as with 100-W power Fig. 2(d)]. This explains why the signal from metallic lead is relatively high in the $4f$ spectrum containing the oxide (Fig. 5). The anisotropy parameter of the $4f$ level ionization at 250 eV has, to the best of our knowledge, not been measured. However, at this photon energy the calculated ionization cross section[45] is already well out of the minimum (at 170 eV) and approaches its flat part. Hence, also the anisotropy parameter should not change much in this region and is close to the low value for higher energies, that is ≈0.3,[45] which is a bit less than the for $5d$ for the photon energies we use. Thus, the $4f$ spectrum shape is consistent with the conclusions based on the comparison of the PAD for the other two levels of lead.

The $4f$ binding energy of the metallic peak in the oxide-containing clusters decreases somewhat and might be below the macroscopic solid-state limit reported in some works. However, for the $4f$ level, this latter value is established with a lower reliability than for the $5d$. The lower $4f$ energy in the oxidized clusters could, in principle, mean that they are, on the whole, negatively charged, which is not impossible considering that the aggregation process takes place in the electron-rich plasma, that oxygen is introduced into the discharge, and that input power is higher than in the $5d$ and valence studies. An alternative explanation can be—considering the limited accuracy of our knowledge on the infinite solid $4f$ ionization potential relative to the vacuum level—that clusters become larger when oxygen is added. As shown above, this should indeed be the case. In fact, a similar negative shift of the metallic peak is also seen in the $5d$ spectra of the oxidized clusters. A third explanation can be that the energy level changes somewhat due to the coordination of the atoms of the metallic surface to the oxide-containing core.

Apart from the binding energy shift, this can also lead to some broadening of metallic peaks in such clusters.

IV. CONCLUSIONS

In summary, complex clusters of a mixed composition containing radially segregated metallic and metal-oxide layers have been produced, and their electronic structure has been disclosed and studied in the present work. Conclusions on the geometric structure have been possible to make analyzing the core and valence photoelectron spectroscopy results obtained using synchrotron radiation as an ionization source. The core-shell structure of the clusters with metallic lead dominating the one to two surface layers has been disclosed using the PAD of different electronic levels. Such a result—opposite to a common situation with the oxide layer on the surface of a metal—has been explained by the peculiarities of the nanoparticle formation process and by the bonding strength differences defining the segregation in the self-assembling process. It is worth emphasizing here that the formation of such a stoichiometry is the interplay of sufficient mobility (or fast kinetics) and thermodynamic mechanisms. For the lead/lead-oxide system in the present case, both kinetics and thermodynamics are rather complex and can be, to a large degree, only speculated about. The kinetics that can facilitate the metallic layer covering the oxide interior is rather likely to be realized in the magnetron discharge plasma of the cluster source. The fact that kinetics is crucial is seen in the differences of the metallic overlayer thickness defined by the oxygen concentration. The lower O_2 fraction leads to an earlier oxidation stop and to a larger number of unoxidized Pb atoms left. The clusters on their way toward the cryostat exit have enough time to be covered by more than one or only one layer of metal. The range of conditions where the overlayer is metallic is rather narrow, but the present method allows us to monitor the situation and to tune the conditions in a sufficiently sensitive way.

As for the thermodynamics, apart from the competition between the metal and the oxide surface energies related to the bond strengths within a compound, it is also the interface energy minimization that plays a role in the cluster formation process. The latter defines, to a great extent, whether there is a well-separated shell of one of the subcomponents or a gradual gradient of their concentrations. In the studies of the formation of the interface between lead and lead oxide,[46] the authors have shown that one of the probable situations is the epitaxial-like boundary that makes the interface energy substantially lower than in the case of disordered or mismatched interfaces. In other words, this means that a clear separation between two components—lead and lead oxide—would be energetically more favorable. The cluster growth mechanism in the present work can lead to a boundary of a similar type although the order of components is reversed. Summing up, one can say that both kinetic and thermodynamic arguments support our conclusions on the core-shell structure with a metallic surface layer over the oxide interior realized in a certain range of clustering conditions.

ACKNOWLEDGMENTS

C.Z. would like to acknowledge the China Scholarship Council (CSC) and National University of Defense Technology (NUDT) for the graduate fellowship. The work presented here has been supported by the Swedish Research Council (VR), the Göran Gustafsson Foundation, the Knut and Alice Wallenberg Foundation, the Crafoord Foundation, Nordforsk, and the Swedish Foundation for Strategic Research. We would also like to thank the MAX-lab staff for their assistance during the experiments.

[1] M. Willander *et al.*, Nanotechnology **20**, 332001 (2009).
[2] H. Liu, S. Wang, G. Zhou, J. Wu, and W. Duan, J. Chem. Phys. **126**, 134705 (2007).
[3] X. Li and L.-S. Wang, Phys. Rev. B **65**, 153404 (2002).
[4] J. Cuppens, C. P. Romero, P. Lievens, and M. J. Van Bael, Phys. Rev. B **81**, 064517 (2010).
[5] S. Bose, C. Galande, S. P. Chockalingam, R. Banerjee, P. Raychaudhuri, and P. Ayyub, J. Phys.: Condens. Matter **21**, 205702 (2009).
[6] A. Sarkar, R. Chadha, T. Mukherjee, and S. Kapoor, Chem. Phys. Lett. **473**, 111 (2009).
[7] S. R. Desai, H. Wu, C. M. Rohlfing, and L.-S. Wang, J. Chem. Phys. **106**, 1309 (1997).
[8] K. S. Kim, T. J. O'Leary, and N. Winograd, Anal. Chem. **45**, 2214 (1973).
[9] V. Senz *et al.*, Phys. Rev. Lett. **102**, 138303 (2009).
[10] S. Osmekhin, M. Tchaplyguine, M.-H. Mikkelä, M. Huttula, T. Andersson, O. Björneholm, and S. Aksela, Phys. Rev. A **81**, 023203 (2010).
[11] B. Wang, J. Zhao, X. Chen, D. Shi, and G. Wang, Phys. Rev. A **71**, 033201 (2005).
[12] H. Li, Y. Ji, F. Wang, S. F. Li, Q. Sun, and Y. Jia, Phys. Rev. B **83**, 075429 (2011).
[13] Z. Zhu, F. F. Tao, F. Zheng, R. Chang, Y. Li, L. Heinke, Z. Liu, M. Salmeron, and G. A. Somorjai, Nano Lett. **12**, 1491 (2012).
[14] S. Andersson, P. A. Brühwiler, A. Sandell, M. Frank, J. Libuda, A. Giertz, B. Brena, A. Maxwell, M. Bäumer, H. J. Freund, and N. Mårtensson, Surf. Sci. **442**, L964 (1999).
[15] Z. Song, J. Hrbek, and R. Osgood, Nano Lett. **5**, 1327 (2005).
[16] X. Y. Kong, Y. Ding, and Z. L. Wang, J. Phys. Chem. B **108**, 570 (2004).
[17] A. Kolmakov, Y. Zhang, and M. Moskovits, Nano Lett. **3**, 1125 (2003).
[18] J.-S. Lee, S.-K. Sim, K.-H. Kim, K. Cho, and S. Kim, Mater. Sci. Eng. B **122**, 85 (2005).
[19] M. Tchaplyguine, S. Legendre, A. Rosso, I. Bradeanu, G. Öhrwall, S. E. Canton, T. Andersson, N. Mårtensson, S. Svensson, and O. Björneholm, Phys. Rev. B **80**, 033405 (2009).
[20] A. Lindblad, H. Bergersen, T. Rander, M. Lundwall, G. Ohrwall, M. Tchaplyguine, S. Svensson, and O. Björneholm, Phys Chem Chem Phys **8**, 1899 (2006).

[21]M. Tchaplyguine, M. Lundwall, M. Gisselbrecht, G. Öhrwall, R. Feifel, S. Sorensen, S. Svensson, N. Mårtensson, and O. Björneholm, Phys. Rev. A **69**, 031201(R) (2004).
[22]A. Lindblad, T. Rander, I. Bradeanu, G. Öhrwall, O. Björneholm, M. Mucke, V. Ulrich, T. Lischke, and U. Hergenhahn, Phys. Rev. B **83**, 125414 (2011).
[23]G. Öhrwall, M. Tchaplyguine, M. Gisselbrecht, M. Lundwall, R. Feifel, T. Rander, J. Schulz, R. R. T. Marinho, A. Lindgren, S. L. Sorensen, S. Svensson, and O. Björneholm, J. Phys. B **36**, 3937 (2003).
[24]D. Rolles, H. Zhang, Z. Pesic, J. Bozek, and N. Berrah, Chem. Phys. Lett. **468**, 148 (2009).
[25]H. Zhang, D. Rolles, Z. D. Pesic, J. D. Bozek, and N. Berrah, Phys. Rev. A **78**, 063201 (2008).
[26]V. Schmidt, *Electron Spectrometry of Atoms Using Synchrotron Radiation* (Cambridge University Press, Cambridge, 1997).
[27]H. Haberland, J. Vac. Sci. Technol. A **12**, 2925 (1994).
[28]M. Hoffmann, G. Wrigge, and B. Issendorff, Phys. Rev. B **66**, 041404(R) (2002).
[29]O. Björneholm, G. Öhrwall, and M. Tchaplyguine, Nucl. Instrum. Methods Phys. Res., Sect. A **601**, 161 (2009).
[30]M. Tchaplyguine, S. Peredkov, A. Rosso, I. Bradeanu, G. Öhrwall, S. Legendre, S. Sorensen, N. Mårtensson, S. Svensson, and O. Björneholm, J. Electron Spectrosc. Relat. Phenom. **166–167**, 38 (2008).
[31]T. Andersson, C. Zhang, A. Rosso, I. Bradeanu, S. Legendre, S. E. Canton, M. Tchaplyguine, G. Öhrwall, S. L. Sorensen, S. Svensson, N. Mårtensson, and O. Björneholm, J. Chem. Phys. **134**, 094511 (2011).
[32]S. Peredkov, S. L. Sorensen, A. Rosso, G. Öhrwall, M. Lundwall, T. Rander, A. Lindblad, H. Bergersen, W. Pokapanich, S. Svensson, O. Björneholm, N. Mårtensson, and M. Tchaplyguine, Phys. Rev. B **76**, 081402(R) (2007).
[33]S. Venkataraj, O. Kappertz, R. Drese, C. Liesch, R. Jayavel, and M. Wuttig, Phys. Status Solidi A **194**, 192 (2002).
[34]G. Makov, A. Nitzan, and L. E. Brus, J. Chem. Phys. **88**, 5076 (1988).
[35]S. Rondon and P. M. A. Sherwood, Surf. Sci. Spectra **5**, 83 (1998).
[36]S. Evans and J. M. Thomas, J. Chem. Soc., Faraday Trans. 2 **71**, 313 (1975).
[37]M. O. Krause, P. Gerard, A. Fahlman, T. A. Carlson, and A. Svensson, Phys. Rev. A **33**, 3146 (1986).
[38]H. Derenbach, H. Kossmann, R. Malutzki, and V. Schmidt, J. Phys. B **17**, 2781 (1984).
[39]R. Morel, A. Brenac, P. Bayle-Guillemaud, C. Portemont, and F. La Rizza, Eur. Phys. J. D **24**, 287 (2003).
[40]S. H. Overbury, P. A. Bertrand, and G. A. Somorjai, Chem. Rev. **75**, 547 (1975).
[41]J. F. Moulder, W. F. Stickle, P. E. Sobol, and K. D. Bomben, *Handbook of X-Ray Photoelectron Spectroscopy: A Reference Book of Standard Spectra for Identification and Interpretation of XPS Data* (Physical Electronics, Chanhassen, MN, 1992), p. 261.
[42]S. Rondon and P. M. A. Sherwood, Surf. Sci. Spectra **5**, 104 (1998).
[43]S. Rondon and P. M. A. Sherwood, Surf. Sci. Spectra **5**, 90 (1998).
[44]S. Rondon and P. M. A. Sherwood, Surf. Sci. Spectra **5**, 97 (1998).
[45]J. J. Yeh and I. Lindau, At. Data Nucl. Data Tables **32**, 1 (1985).
[46]A. W. D. Van Der Gon, B. Pluis, R. J. Smith, and J. F. Van Der Veen, Surf. Sci. **209**, 431 (1989).